Available online at www.sciencedirect.com
SCIENCE DIRECT®
Inorganica Chimica Acta 347 (2003) 137–144
Inorganica Chimica Acta
www.elsevier.com/locate/ica

Sulfido–carbonyl ruthenium clusters derived from tertiary phosphine sulfides

Daniele Belletti, Claudia Graiff, Virginia Lostao, Roberto Pattacini, Giovanni Predieri, Antonio Tiripicchio *

Dipartimento di Chimica Generale ed Inorganica, Chimica Analitica, Chimica Fisica, Università di Parma, Parco Area delle Scienze 17/A, I-43100 Parma, Italy

Received 15 May 2002; accepted 24 July 2002

Dedicated to the extraordinary and long career of Professor Rafael Usón, which has accompanied all the growth of Spanish Organometallic Chemistry

Abstract

The reactions of $Ru_3(CO)_{12}$ with 2,4,6 tris-(trimethoxy)phenylphosphino sulfide (ttmppS) and with 1,2 bis-[(diphenylphosphino)methyl]benzene disulfide ($dpmbS_2$) afford a variety of phosphine substituted sulfido carbonyl clusters. These belong to three different families of clusters showing, respectively, (i) the Ru_3S (compound **4**), (ii) the Ru_3S_2 (compound **3**), and (iii) the Ru_4S_2 cores (compounds **1** and **2**). Similar distributions of products have been observed in the case of the reactions between $M_3(CO)_{12}$ (M = Ru or Fe) and phosphine and diphosphine selenides. The structures of complexes **1**–**4** have been determined by X-ray diffraction methods.

Keywords: Sulfido complexes; Ruthenium complexes; Crystal structures; Cluster complexes

1. Introduction

The chemistry of transition-metal sulfido, selenido and tellurido mono- and polynuclear complexes is a research area of increasing interest, as pointed out in recent reviews [1–3]. The reasons for this growing interest derive from the usefulness of these ligands in cluster growth reactions and from the search for precursors of nanoparticles with novel electronic, magnetic and optical properties [3,4], considering the size-dependence of physico-chemical properties of substances such as metals and semiconductors [5,6].

In recent years we have carried out systematic investigations on the selenium transfer reactions by tertiary phosphine and diphosphine selenides, namely Ph_3PSe, (tppSe), $CH_2(Ph_2PSe)_2$, (dppmSe$_2$), $(CH_2Ph_2PSe)_2$, (dppeSe$_2$), $Fe(\eta^5\text{-}C_5H_4Ph_2PSe)_2$, (dppfcSe$_2$), towards iron and ruthenium carbonyl clusters [7]. These reactions take advantage of the frailty of the P=Se bond and provide a simple, sometimes selective [8] synthetic route to phosphine-substituted, mono- and diselenido trinuclear clusters. Further pyrolytic processes usually lead to the formation of tetrahedral species M_2Se_2, in the case of iron, and octahedral species M_4Se_2, in the case of ruthenium (see Scheme 1). Occasionally, other less common compounds can be obtained via condensation processes such as clusters containing butterfly M_6Se_4 cores [9] (represented in Scheme 1) and the cubane-like cage complex $[Ru_4(\mu_3\text{-Se})_4(CO)_{10}(\mu\text{-dppm})]$ [10].

Continuing these investigations, we have recently observed that tertiary phosphine selenides bearing heterocyclic fragments, such as 2-thienyl (th), 2-pyridyl (py) and 5-(2-pyridyl)-2-thienyl (pyth), can undergo P–C bond cleavage by reaction with iron and ruthenium carbonyl clusters. Actually in the case of Ph_2(th)PSe and Ph_2(py)PSe with ruthenium, the addition is not only limited to the transfer of the chalcogenido atom, but proceeds with P–C bond cleavage, affording selenido–

* Corresponding author. Fax: +39-0521-905-557.
E-mail address: tiri@unipr.it (A. Tiripicchio).

0020-1693/02/$ - see front matter © 2002 Elsevier Science B.V. All rights reserved.
doi:10.1016/S0020-1693(02)01455-X

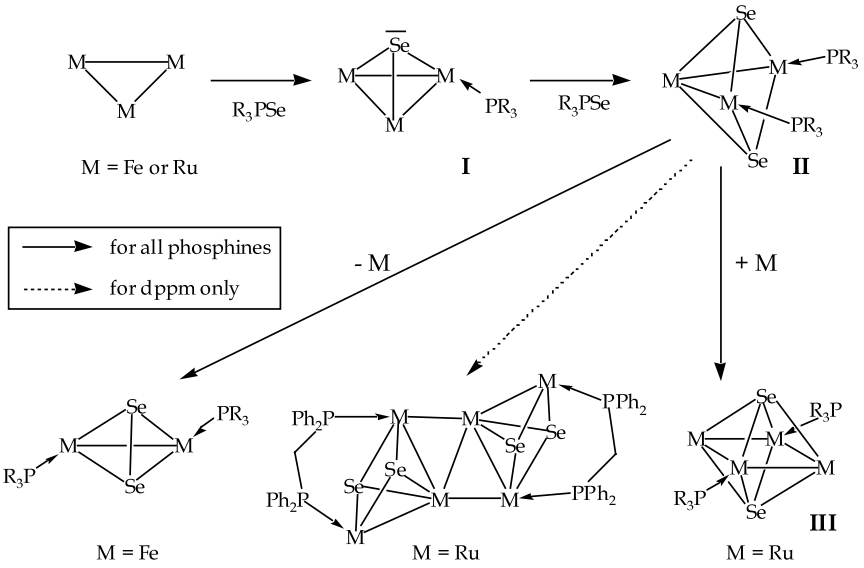

Scheme 1.

phosphido clusters [11,12]. In particular in the case of the thienyl group, the 48-electron cluster $[Ru_3(\mu_3\text{-}Se)(\mu\text{-}PPh_2)(\mu\text{-th})(CO)_6\{P(th)Ph_2\}]$ has been obtained in good yields by a one step synthesis. Its molecular structure shows the contemporary presence of the diphenylphosphido (bridging one side) and selenido (capping) ligands on the same cluster core [13].

Finally we have reacted different phosphine selenides with the tetrahedral clusters $[HMCo_3(CO)_{12}]$ (M = Fe or Ru) in order to obtain new chalcogenido–carbonyl bimetallic clusters [14] considering that the presence of different metals can influence the selectivity of certain processes [15,16] and lead to the formation of compounds presenting new and not always easily predictable structures.

As a natural extension of these investigations, we have decided to react carbonyl metal clusters such as $M_3(CO)_{12}$ (M = Fe or Ru) with tertiary phosphine sulfides with the aim to observe the transfer of sulfur atoms to zero-valent metal complexes leading to sulfido carbonyl ruthenium clusters substituted by tertiary phosphines. Previous investigations on the reactions of phosphine sulfides with carbonyl complexes involved Ph_3PS [17], $Ph_2P(S)H$ [18], $\{PhP(S)\}_2CH_2$ and PhP(S)C≡CR [19].

This paper deals with the reactions between $Ru_3(CO)_{12}$ and mono- and diphosphine sulfides such as 2,4,6 tris-(trimethoxy)phenylphosphino sulfide (ttmppS) and 1,2 bis-[(diphenylphosphino)methyl] benzene disulfide ($dpmbS_2$) and with the characterization of the derived sulfido–carbonyl ruthenium clusters. As regards the dpmb diphosphine, even if its preparation has been reported several years ago [20], nevertheless its coordination chemistry appears to have been little investigated. In particular it has been utilized as ligand in the synthesis of Pd, [21,22] Pt, [23–25] Ni, [25] and Ag [26] complexes, where the diphosphine acts mostly as a chelating ligand bearing to the formation of stable seven membered chelating rings, whose conformations have been studied in solid state as well as in solution.

2. Experimental

2.1. General

The starting reagents $Ru_3(CO)_{12}$, sulfur and tertiary phosphines were pure commercial products (Aldrich and Fluka) and were used as received. The solvents (C. Erba) were dried and distilled by standard techniques before use. All manipulations (prior to the TLC separations) were carried out under dry nitrogen by means of standard Schlenk-tube techniques. Elemental (C, H, S) analyses were performed with a Carlo Erba EA 1108 automated analyzer. IR spectra (KBr discs or CH_2Cl_2 solutions) were recorded on a Nicolet 5PC FT or a Nicolet Nexus FT spectrometer. ^1H (300 MHz), ^{31}P (81.0 MHz, 85% H_3PO_4 as external reference) NMR spectra ($CDCl_3$ solutions) were recorded on Bruker instruments AC 300 (^1H) and CXP 200 (^{31}P).

Mass spectra were obtained using a Finnigan MAT SSQ710 spectrometer equipped with an IC/CI source, a direct inlet system and a quadrupole mass analyzer was used. The CI source was utilized with methane as the reagent gas (T source, 220 °C; methane ionization energy, 70 eV). The quadrupole temperature was maintained at 140 °C; the system was scanned from 400 to 1600 a.m.u. and negative ion (NICI) spectra were recorded.

2.2. Preparation and reactions

2.2.1. Preparation of the phosphine sulfides

The ligands ttmppS and dpmbS_2 were prepared by elemental sulfur transfer.

A toluene suspension (20 ml) of elemental sulfur (30 mg, 0.94 mmol) was added to a solution of 500 mg (0.94 mmol) of ttmpp in 25 ml of toluene. The mixture was refluxed for 5 h. The solvent was removed in vacuo and the rough powder was used as obtained. Yield 85%. *Anal.* Found: C, 57.41; H, 5.85; S, 5.62. $C_{27}H_{33}O_9PS$ Calc.: C, 57.44; H, 5.89; S, 5.68%. FTIR (KBr) (cm^{-1}): 682 s, 660 vs (νP=S). ^{1}H NMR ($CHCl_3$-d_1): d 6.03 (d, $^2J_{(H,P)}$ 4Hz, 6Har), 3.77 (s, 9H, *p*-Me), 3.53 (s, 18H, *o*-Me). ^{31}P NMR ($CHCl_3$-d_1): 11.3 (s). MS NICI, *m/z* (%):564 $(ttmppS)^-$ (100); 532 $(ttmp)^-$, (15); 365 $(2,4,6\ tris\ OCH_3\text{-}C_6H_2)_2P)^-$, (40).

20 ml of a toluene suspension of elemental sulfur (67 mg, 2.10 mmol) was added to a solution of 500 mg (1.05 mmol) of dpmb. The mixture was refluxed for 6 h. The solvent was removed and the rough powder was used as obtained. Yield 87%. *Anal.* Found: C, 71.41; H, 5.21; S, 11.81. $C_{32}H_{28}P_2S_2$ Calc.: C, 71.36; H, 5.24; S, 11.90%. FTIR (KBr) (cm^{-1}): 602 vs (νP=S). ^{1}H NMR ($CHCl_3$-d_1): d 7.81–7.32 (m, 20H, Ph), 6.86 (m, 2Har), 6.55 (m, 2Har), 3.99 (d, $^2J_{(H,P)}$ 11Hz, 4H). ^{31}P NMR ($CHCl_3$-d_1): 39.1 (s). MS–NICI, *m/z* (%): 538 $(dpmbS_2)^-$ (70); 321 $(PCH_2(C_6H_4)CH_2PPh_2)^-$, (100); 217 $(Ph_2PS)^-$, (40).

2.2.2. Reaction of ttmppS with $Ru_3(CO)_{12}$

$Ru_3(CO)_{12}$ (300 mg, 0.47 mmol) and ttmppS (264 mg, 0.47 mmol, 1:1 molar ratio) were reacted in hot toluene (100 ml) at 50 °C for about 1.5 h, in the presence of Me_3NO (35 mg), under nitrogen atmosphere. The deep red solution was evaporated to dryness and the residue was disolved in a small amount of CH_2Cl_2. Preparative TLC (Kieselgel P.F. Merck, eluant mixture tetrahydrofuran/toluene 2:1) yielded a red band together with other unresolved bands and some decomposition. The red band contained the *closo* cluster $[Ru_4(\mu_4\text{-}S)_2(CO)_8(\mu\text{-}CO)_2P\{(2,4,6\ OCH_3)_3(C_6H_2)\}_3]$ (**1**, yield 20%), identified by X-ray diffraction methods.

Cluster **1**: IR (CH_2Cl_2, νCO, cm^{-1}): 2060s, 2020vs, 1984m, 1869w, 1828w. ^{1}H NMR ($CHCl_3$-d_1): 5.89 (d, $^2J_{(H,P)}$ 4Hz, 6Har), 3.76 (s, 9H, *p*-Me), 3.58 (s, 18H, *o*-Me). *Anal.* Found: C, 35.11; H, 2.62; S, 5.02. $Ru_4S_2PO_{19}C_{37}H_{33}$ Calc.: C, 34.69; H, 2.59; S, 5.00%.

2.2.3. Reaction of dpmbS_2 with $Ru_3(CO)_{12}$

$Ru_3(CO)_{12}$ (300 mg, 0.47 mmol) and dpmbS_2 (252 mg, 0.47 mmol, 1:1 molar ratio) were reacted in hot toluene (100 ml) at 70 °C for about 3 h, in the presence of Me_3NO (35 mg), under nitrogen atmosphere. The deep red solution was evaporated to dryness and the residue was dissolved in a small amount of CH_2Cl_2. Preparative TLC (Kieselgel P.F. Merck, eluant mixture CH_2Cl_2/hexane 1:1) yielded a orange band, a yellow one, a red one and two deep red bands together with some decomposition. The red band and the two deep red bands contained, respectively, the *closo* cluster $[Ru_4(\mu_4\text{-}S)_2(CO)_8(\mu\text{-}CO)(\mu\text{-}dpmb)]$ (**2**, yield 15%), the *nido* cluster $[Ru_3(\mu_3\text{-}S)_2(CO)_7(dpmb)]$ (**3**, yield 30%) and the monosulfido cluster $[Ru_3(\mu_3\text{-}S)\{\mu\text{-}P(Ph)CH_2C_6H_4\text{-}CH_2PPh_2\}(\mu\text{-}OCPh)(CO)_6]$ (**4**, yield 2%), whose structures have been determined by spectroscopic and X-ray diffraction methods.

Cluster **2**: IR (CH_2Cl_2, νCO, cm^{-1}): 2048s, 2017vs, 1999vs, 1974s, 1824w. ^{1}H NMR ($CHCl_3$-d_1): 7.61–6.89 (m, 20Har), 6.20–5.59 (m, 4Har), 3.75 (m, 4H, CH_2). *Anal.* Found: C, 41.25; H, 2.45; S, 5.42. $Ru_4S_2P_2O_9C_{41}H_{28}$ Calc.: C, 41.20; H, 2.36; S, 5.36%.

Cluster **3**: IR (CH_2Cl_2, νCO, cm^{-1}): 2074vs, 2041vs, 1999sh, 1995s, 1946w. ^{1}H NMR ($CHCl_3$-d_1): 7.93–6.66 (m, 20Har), 6.23 (m, 2Har), 5.87 (m, 2Har), 4.37 (m, 2H, CH_2) 3.85 (m, 2H, CH_2). *Anal.* Found: C, 45.41; H, 2.85; S, 6.12. $Ru_3S_2P_2O_7C_{39}H_{28}$ Calc.: C, 45.13; H, 2.72; S, 6.18%.

Cluster **4**: IR (CH_2Cl_2, νCO, cm^{-1}): 2038m, 2020vs, 1993s, 1968sh. ^{31}P NMR ($CHCl_3$-d_1): 218.2 (s), 33.2 (s). *Anal.* Found: C, 46.01; H, 2.86; S, 3.14. $Ru_3S\text{-}P_2O_7C_{39}H_{28}$ Calc.: C, 46.58; H, 2.80; S, 3.19%.

2.3. X-ray data collection, structure solution and refinement for complexes ***1***·0.5$CHCl_3$, ***2***·0.5CH_2Cl_2, ***3*** and ***4***

The intensity data were collected at room temperature on a Bruker AXS Smart 1000 diffractometer, equipped with an area detector using a graphite monochromated Mo Kα radiation. The SMART program package was used to determine the unit-cell parameters and for data collection. Crystallographic and experimental details for structures are summarized in Table 1.

The poor quality of the crystals of cluster **4** prevented accurate results of the structure determination. The structures were solved by Patterson and Fourier methods and refined by full-matrix least-squares procedures (based on F_o^2) [27–30] with anisotropic thermal parameters in the last cycles of refinement for all the non-hydrogen atom excepting for the carbon and chlorine atoms of the solvent molecules in **1** and **2** and the carbon and oxygen atoms of the molecule in compound **4**. In the crystals of **1** and **2** molecules of $CHCl_3$ and CH_2Cl_2, respectively, were found with occupancy factor 0.5.

In the structures the hydrogen atoms were introduced into the geometrically calculated positions and refined riding on the corresponding parent atoms, excepting for those of the solvents. In the final cycles of refinement a weighting scheme $w = 1/[\sigma^2F_o^2 + (0.1363P)]$ (**1**), $w = 1/[\sigma^2F_o^2 + (0.0487P)^2]$ (**2**), $w = 1/[\sigma^2F_o^2 + (0.0273P)^2]$ (**3**) and $w = 1/[\sigma^2F_o^2 + (0.0001P)^2 + 179.9571]$ (**4**), where $P = (F_o^2 + 2F_c^2)/3$, was used.

Table 1
Crystal data and structure refinement for compound **1**·0.5$CHCl_3$, **2**·0.5CH_2Cl_2, **3**, **4**

Compound	**1**·0.5$CHCl_3$	**2**·0.5CH_2Cl_2	**3**	**4**
Formula	$Ru_4S_2PO_{19}C_{37}H_{33}\cdot 1/2CHCl_3$	$Ru_4S_2P_2O_9C_{41}H_{28}\cdot 1/2CH_2Cl_2$	$Ru_3S_2P_2O_7C_{39}H_{28}$	$Ru_3SP_2O_7C_{39}H_{28}$
Formula weight	1340.69	1237.44	1037.88	1005.82
Crystal system	monoclinic	monoclinic	monoclinic	triclinic
Space group	$C2/c$	$P2_1/n$	$P2_1/c$	$P\bar{1}$
Unit cell dimensions				
a (Å)	20.214(4)	14.157(4)	11.383(4)	10.135 (4)
b (Å)	18.005(4)	19.412(4)	18.872(5)	11.219(3)
c (Å)	29.628(4)	16.348(4)	18.973(3)	17.818(5)
α (°)	90	90	90	98.82(5)
β (°)	103.73(3)	100.85(3)	102.13(3)	92.27(3)
γ (°)	90	90	90	93.10(5)
V (Å^3)	10475(3)	4412(2)	3985(2)	1997(1)
Z	8	4	4	2
D_{calc} (Mg m^{-3})	1.700	1.863	1.730	1.673
Absorption coefficient (cm^{-1})	13.84	16.24	13.55	12.99
$F(000)$	5272	2420	2048	992
Crystal size (mm^3)	0.18 × 0.32 × 0.37	0.22 × 0.13 × 0.22	0.14 × 0.20 × 0.19	0.11 × 0.25 × 0.25
θ Range (°)	1.42–27.02	1.65–27.01	1.54–27.02	1.84–23.32
Reflections collected	56876	26338	23881	4485
Independent reflections	11408 [$R_{int} = 0.0599$]	9526 [$R_{int} = 0.0508$]	8618 [$R_{int} = 0.0708$]	3929 [$R_{int} = 0.0339$]
Observed reflections [$I > 2\sigma(I)$]	7137	5228	3966	1893
Data/restr./param.	11408/0/588	9526/0/541	8618/0/485	3929/0/245
Goodness-of-fit on F^2	1.021	0.918	0.797	1.067
Final R indices [$I > 2\sigma(I)$]	$R_1 = 0.0537$, $wR_2 = 0.1903$	$R_1 = 0.0393$, $wR_2 = 0.0927$	$R_1 = 0.0409$, $wR_2 = 0.0692$	$R_1 = 0.1073$, $wR_2 = 0.2131$
R indices (all data)	$R_1 = 0.0967$, $wR_2 = 0.2159$	$R_1 = 0.0981$, $wR_2 = 0.1089$	$R_1 = 0.1239$, $wR_2 = 0.0849$	$R_1 = 0.2386$, $wR_2 = 0.3024$
Largest difference peak and hole (e Å^{-3})	2.283 and −0.795	0.645 and −0.696	0.690 and −0.551	1.207 and −1.194

$R_1 = \Sigma||F_o|-|F_c||/\Sigma|F_o|$. $wR_2 = [\Sigma[w(F_c^2-F_o^2)^2]/\Sigma[w(F_o^2)^2]]^{1/2}$.

All calculations were carried out on Digital AlphaStation 255 computers.

3. Results and discussion

3.1. Synthesis and spectroscopic characterization of the compounds

The reactions of $Ru_3(CO)_{12}$ with different phosphine sulfides, in hot toluene and in the presence of Me_3NO as decarbonylating agent, produce a variety of phosphine-substituted sulfido–carbonyl clusters, whose structural frameworks are analogous to those found for phosphine-substituted selenido carbonyl clusters [7]. They are air stable, colored solids and have been isolated by TLC on silica gel [31] and characterized by spectroscopic data. In some cases their slow crystallization allows to obtain single crystals suitable for X-ray diffraction analysis. In particular we obtained workable amounts of cluster **3** (structure **II** of Scheme 1) showing a Ru_3S_2 core. This cluster belongs to the family of 50-electron nido clusters with seven skeletal electron pairs; these clusters are usually the main products of this kind of reactions as observed in the case of selenium/ruthenium, and selenium/iron carbonyl compounds [7,8]. Cluster **3** could be described as a square pyramid with two metal and two sulfur atoms alternating in the basal plane and the third metal atom at the apex of the pyramid. The dpmb chelates one of the ruthenium atoms at the base of the pyramid.

On the other hand, clusters **1** and **2** belong to the family of Ru_4S_2 62 electron *closo* clusters with seven skeletal electron pairs (structure **III** of Scheme 1). **1** is the unique product isolable from the reaction between $dpmbS_2$ and $Ru_3(CO)_{12}$.

Clusters **1**, **2** and **3** are substituted sulfido metal carbonyl clusters, in which sulfur atoms are transferred to the metal core and one or two carbonyl groups are substituted by a mono or a diphosphine. It is interesting to note that in this kind of reactions, carried out at 70 °C, the pyrolytic fragmentation of the dpmb occurs leading to the rupture of a P–C(Ph) bond with release of a phenyl group. This undergo CO migratory insertion affording a benzoyl fragment bridging two Ru atoms as reported in the description of the crystal structure (see below). The same behaviour has been observed in the case of the reaction between $Ru_3(CO)_{12}$ and the $dppfcSe_2$, where, among the minor products present in the reaction mixtures, it was possible to isolate few

crystals of the red derivative of formula $[Ru_3(\mu_3\text{-}Se)\{\mu\text{-}P(Ph)C_5H_4FeC_5H_4PPh_2\}(\mu\text{-}OCPh)(CO)_6]$ [32]. This cluster and compound **4** are very similar as they consist of a trinuclear cluster with a Ru_3E *core* (E = Se or S). The chalcogenido atom caps the metal triangle, two sides of which are bridged by a phosphido and a benzoyl group.

3.2. Crystal structure determination of *1·0.5CHCl₃, 2·0.5 CH₂Cl₂, 3 and 4*

Views of the structures of **1** and **2** are shown in Figs. 1 and 2 together with atomic numbering scheme; selected bond distances and angles are given in Tables 2 and 3.

Complexes **1** and **2** exhibit a distorted *closo*-octahedral Ru_4S_2 core with seven skeletal electron pairs. In **1** two carbonyls asymmetrically bridge two adjacent Ru–Ru edges, which are the shortest of the four Ru–Ru edges (Ru2–Ru3 and Ru3–Ru4 2.749(1), 2.748(1) Å, respectively) as observed in many chalcogenido metal clusters containing bridging carbonyl groups [7,33,34]. All the ruthenium atoms are also bound to two terminal carbonyls, whereas the phosphine ligand is bound to the Ru1 atom. The Ru1–P1 bond length, 2.401(2) Å, is slightly longer of that found in the analogous selenium cluster $[Ru_4(\mu_4\text{-}Se)_2(CO)_8(\mu\text{-}CO)_2P(C_6H_5)_3]$ [2.329(7) and 2.338(7) Å, respectively, for the two independent molecules] [34]. The Ru–S bond lengths span from 2.452(2) to 2.527(2) Å, while the S···S separation is of 3.050(3) Å, in good agreement with the averaged values found in the Ru_4S_2 clusters (3.08 Å) [7].

In 2 a carbonyl group bridges a Ru–Ru edge, which is the shortest of the four Ru–Ru edges (Ru3–Ru4 2.741(1) Å) [7,33]. All the ruthenium atoms are also bound to two terminal carbonyls. The diphosphine bridges the longest Ru–Ru edge (2.834(1) Å), forming an eight membered ring. If the xylene moiety is excluded the Ru1,Ru2,P1,P2,C17,C10 atoms adopt a boat conformation with P1 and P2 deviated respectively of +0.204(2) and +0.261(2) Å from the mean plane defined by Ru1,Ru2,C10,C17; this plane forms a dihedral angle of 85.3(1)° with the xylene moiety (mean plane defined by C10,C11,C12,C13,C14,C15,C16,C17) and a dihedral angle of 53.0(1)° with the mean plane defined by the four metal atoms Ru1,Ru2,Ru3,Ru4. The presence of the bridging ligand with a large bite (xylene moiety) promotes the elongation of the Ru1–Ru2 edge [7,33]. The Ru–S bond distances span from 2.459(2) to 2.511(2) Å in good agreement with those found in **1**. The S···S separation is of 3.048(2) Å [7].

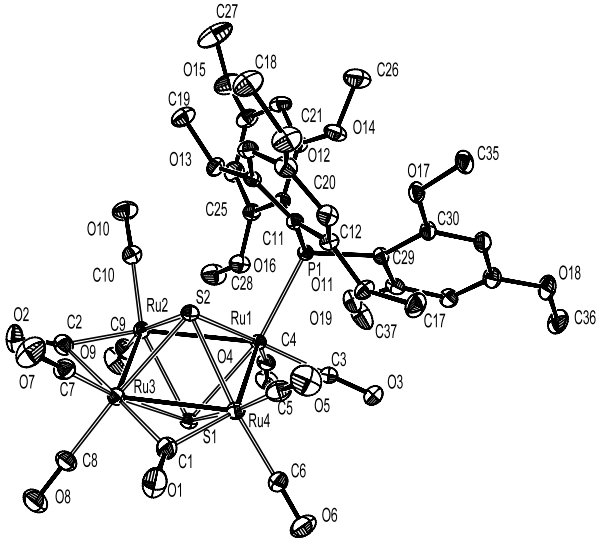

Fig. 1. View of the molecular structure of cluster **1** with the atomic labelling scheme. The thermal ellipsoids are drawn at the 30% probability level.

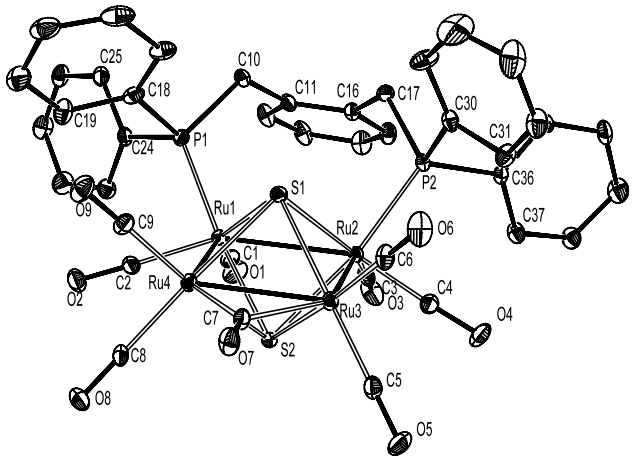

Fig. 2. View of the molecular structure of cluster **2** with the atomic labelling scheme. The thermal ellipsoids are drawn at the 30% probability level.

Table 2
List of bond lengths (Å) and bond angles (°) for **1**·0.5CHCl₃

Bond lengths			
Ru(1)–Ru(2)	2.802(1)	Ru(4)–S(1)	2.464(2)
Ru(1)–Ru(4)	2.819(1)	Ru(4)–S(2)	2.481(2)
Ru(2)–Ru(3)	2.749(1)	Ru(1)–P(1)	2.401(2)
Ru(3)–Ru(4)	2.748(1)	Ru(3)–C(1)	2.139(11)
Ru(1)–S(1)	2.480(2)	Ru(4)–C(1)	2.006(10)
Ru(1)–S(2)	2.508(2)	Ru(3)–C(2)	2.299(11)
Ru(2)–S(1)	2.452(2)	Ru(2)–C(2)	1.984(10)
Ru(2)–S(2)	2.473(2)	O(1)–C(1)	1.166(12)
Ru(3)–S(1)	2.520(2)	O(2)–C(2)	1.157(11)
Ru(3)–S(2)	2.527(2)		
Bond angles			
Ru(2)–Ru(1)–Ru(4)	87.22(3)	S(1)–Ru(3)–S(2)	74.36(7)
Ru(3)–Ru(2)–Ru(1)	91.71(3)	S(1)–Ru(4)–S(2)	76.16(7)
Ru(4)–Ru(3)–Ru(2)	89.71(3)	Ru(2)–S(1)–Ru(4)	104.15(8)
Ru(3)–Ru(4)–Ru(1)	91.36(3)	Ru(1)–S(1)–Ru(3)	105.66(8)
P(1)–Ru(1)–S(1)	166.46(7)	Ru(2)–S(2)–Ru(4)	103.02(7)
P(1)–Ru(1)–S(2)	95.80(7)	Ru(1)–S(2)–Ru(3)	104.59(8)
S(1)–Ru(1)–S(2)	75.39(7)	Ru(4)–C(1)–Ru(3)	83.0(4)
S(1)–Ru(2)–S(2)	76.53(7)	Ru(2)–C(2)–Ru(3)	79.5(4)

Table 3
List of bond lengths (Å) and bond angles (°) for **2**·0.5CH_2Cl_2

Bond lengths			
Ru(1)–Ru(4)	2.780(1)	Ru(4)–S(2)	2.508(2)
Ru(1)–Ru(2)	2.834(1)	Ru(1)–P(1)	2.305(2)
Ru(2)–Ru(3)	2.769(1)	Ru(2)–P(2)	2.309(2)
Ru(3)–Ru(4)	2.741(1)	Ru(3)–C(7)	2.052(6)
Ru(1)–S(1)	2.475(2)	Ru(4)–C(7)	2.045(7)
Ru(1)–S(2)	2.485(2)	P(1)–C(10)	1.843(6)
Ru(2)–S(1)	2.459(2)	P(2)–C(17)	1.833(6)
Ru(2)–S(2)	2.483(2)	O(7)–C(7)	1.159(7)
Ru(3)–S(1)	2.497(2)	C(10)–C(11)	1.497(9)
Ru(3)–S(2)	2.511(2)	C(11)–C(16)	1.405(9)
Ru(4)–S(1)	2.488(2)	C(16)–C(17)	1.506(9)
Bond angles			
Ru(4)–Ru(1)–Ru(2)	88.66(2)	S(1)–Ru(4)–S(2)	75.18(6)
Ru(3)–Ru(2)–Ru(1)	89.42(2)	Ru(2)–S(1)–Ru(4)	104.93(6)
Ru(4)–Ru(3)–Ru(2)	90.79(3)	Ru(1)–S(1)–Ru(3)	104.92(6)
Ru(3)–Ru(4)–Ru(1)	91.13(2)	Ru(2)–S(2)–Ru(4)	103.65(6)
P(1)–Ru(1)–S(1)	94.30(6)	Ru(1)–S(2)–Ru(3)	104.20(6)
P(1)–Ru(1)–S(2)	170.10(6)	C(10)–P(1)–Ru(1)	116.3(2)
P(2)–Ru(2)–S(1)	91.86(6)	C(17)–P(2)–Ru(2)	116.4(2)
P(2)–Ru(2)–S(2)	168.01(6)	Ru(3)–C(7)–Ru(4)	84.0(3)
S(1)–Ru(1)–S(2)	75.83(6)	C(11)–C(10)–P(1)	115.0(5)
S(1)–Ru(2)–S(2)	76.15(6)	C(16)–C(17)–P(2)	116.1(4)
S(1)–Ru(3)–S(2)	74.96(5)		

A view of the structure of **3** is shown in Fig. 3 together with atomic numbering scheme; selected bond distances and angles are given in Table 4.

Compound **3** is a 50-electron *nido* cluster with the well known M_3S_2 core [35,9], which can be described as a square pyramid with two metal and two sulfur atoms alternating in the basal plane and the third metal atom at the apex of the pyramid. The diphosphine chelates

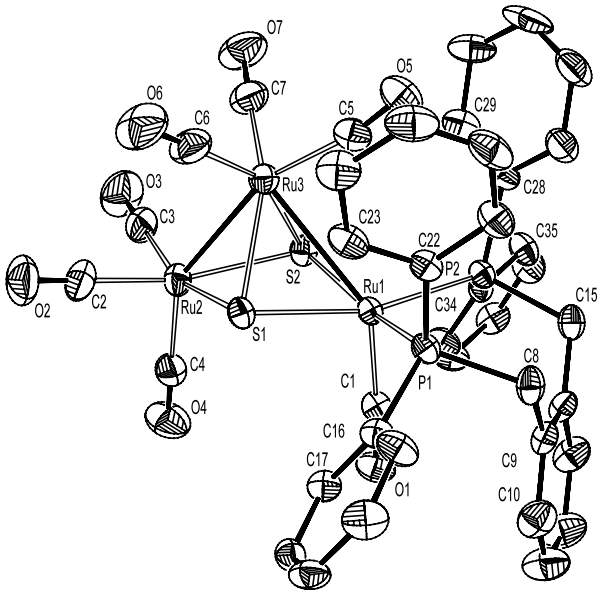

Fig. 3. View of the molecular structure of cluster **3** with the atomic labelling scheme. The thermal ellipsoids are drawn at the 30% probability level.

Table 4
List of bond lengths (Å) and bond angles (°) for **3**

Bond lengths			
Ru(1)–Ru(3)	2.935(1)	Ru(1)–P(1)	2.338(2)
Ru(2)–Ru(3)	2.715(1)	Ru(1)–P(2)	2.337(2)
Ru(1)–S(1)	2.362(2)	P(1)–C(8)	1.832(6)
Ru(1)–S(2)	2.379(2)	P(2)–C(15)	1.837(5)
Ru(2)–S(2)	2.385(2)	C(8)–C(9)	1.500(8)
Ru(2)–S(1)	2.393(2)	C(9)–C(14)	1.407(8)
Ru(3)–S(2)	2.415(2)	C(14)–C(15)	1.502(7)
Ru(3)–S(1)	2.413(2)		
Bond angles			
Ru(2)–Ru(3)–Ru(1)	80.20(3)	S(2)–Ru(2)–S(1)	78.16(5)
Ru(1)–S(1)–Ru(2)	100.01(6)	S(2)–Ru(3)–S(1)	77.20(5)
Ru(1)–S(1)–Ru(3)	75.85(5)	P(2)–Ru(1)–P(1)	97.16(6)
Ru(2)–S(1)–Ru(3)	68.78(5)	C(8)–P(1)–Ru(1)	117.97(19)
Ru(1)–S(2)–Ru(2)	99.77(6)	C(15)–P(2)–Ru(1)	118.61(19)
Ru(1)–S(2)–Ru(3)	75.50(5)	C(9)–C(8)–P(1)	113.4(4)
Ru(2)–S(2)–Ru(3)	68.88(5)	C(14)–C(15)–P(2)	113.8(4)
S(1)–Ru(1)–S(2)	78.90(5)		

one of the metal atoms at the base of the pyramid, Ru1, the two phosphorous atoms substituting two carbonyl groups in equatorial positions; the bond distances Ru1–P1 and Ru1–P2 are 2.337(2) and 2.338(2) Å respectively. The chelation of the diphosphine on Ru1 atom produces a lenghtening of the Ru1–Ru3 side of the cluster [9], 2.935(1) Å, against 2.715(1) Å of the Ru2–Ru3 side. The chelating diphosphine forms with Ru1 a seven-membered ring which presents a boat conformation, with the Ru1, C9 and C14 atoms deviated in the same direction over the mean plane defined by P1,P2,C8,C15 (the deviations for Ru1, C9, C14 atoms are 0.693(1), 1.170(1), 1.200(1) Å, respectively).

A view of the structure of **4** is shown in Fig. 4 together with atomic numbering scheme; selected bond distances and angles are given in Table 5.

It presents a Ru_3S core with the sulfur atom capping the metal triangle, two sides of which are bridged by a

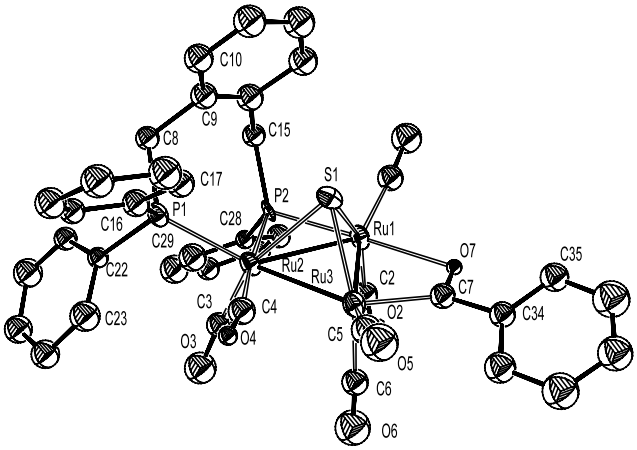

Fig. 4. View of the molecular structure of cluster **4** with the atomic labelling scheme. The thermal ellipsoids are drawn at the 30% probability level.

Table 5
List of bond lengths (Å) and bond angles (°) for **4**

Bond lengths			
Ru(1)–Ru(3)	2.791(4)	Ru(1)–O(7)	2.423(17)
Ru(1)–Ru(2)	2.877(4)	Ru(3)–C(7)	2.01(4)
Ru(2)–Ru(3)	2.696(4)	P(1)–C(8)	1.89(3)
Ru(2)–S(1)	2.459(9)	P(2)–C(15)	1.83(3)
Ru(1)–S(1)	2.410(9)	O(7)–C(7)	1.27(4)
Ru(3)–S(1)	2.422(10)	C(7)–C(34)	1.49(5)
Ru(1)–P(2)	2.358(9)	C(8)–C(9)	1.62(5)
Ru(2)–P(1)	2.384(10)	C(9)–C(14)	1.35(5)
Ru(2)–P(2)	2.424(9)	C(14)–C(15)	1.51(5)
Bond angles			
Ru(3)–Ru(1)–Ru(2)	56.79(11)	P(2)–Ru(2)–Ru(3)	112.0(2)
Ru(3)–Ru(2)–Ru(1)	60.01(11)	P(1)–Ru(2)–Ru(1)	138.0(3)
Ru(2)–Ru(3)–Ru(1)	63.20(11)	P(2)–Ru(2)–Ru(1)	52.0(2)
P(2)–Ru(1)–S(1)	85.4(3)	C(7)–Ru(3)–Ru(1)	75.2(10)
P(2)–Ru(1)–O(7)	175.4(5)	C(8)–P(1)–Ru(2)	119.4(11)
P(2)–Ru(1)–Ru(3)	110.9(2)	C(15)–P(2)–Ru(1)	116.6(12)
O(7)–Ru(1)–Ru(3)	64.8(4)	C(15)–P(2)–Ru(2)	120.4(11)
P(2)–Ru(1)–Ru(2)	54.1(2)	Ru(1)–P(2)–Ru(2)	74.0(3)
O(7)–Ru(1)–Ru(2)	121.5(4)	C(7)–O(7)–Ru(1)	103.9(19)
P(1)–Ru(2)–P(2)	93.8(3)	O(7)–C(7)–C(34)	108.0(3)
P(1)–Ru(2)–S(1)	106.0(3)	O(7)–C(7)–Ru(3)	116.0(2)
P(2)–Ru(2)–S(1)	82.9(3)	C(34)–C(7)–Ru(3)	136.0(3)
P(1)–Ru(2)–Ru(3)	144.0(3)	C(9)–C(8)–P(1)	112.0(2)

phosphide ligand and by a benzoyl group, which derives from the multiple fragmentation of the parent 1,2 bis-[(diphenylphosphino)methyl]benzene disulfide, followed by the migratory insertion of a phenyl ring into a carbonyl group. The two bridged sides of the metal triangle are the longest ones [2.791(4) and 2.877(4) Å] and a semibridging carbonyl [Ru2–C4 1.94(4), Ru3–C4 2.53(4) Å, Ru2–C4–O4 169(4)°] is placed on the shortest side [2.696(4) Å]. The three Ru–S bond distances span from 2.410(9) to 2.459(9) Å. Due to the loss of a phenyl ring the phosphino–phosphido ligand is coordinated to the Ru1 and Ru2 atoms in unusual manner: the phosphido P2 atom asimetrically bridges the Ru1–Ru2 side [Ru1–P2 2.358(9), Ru2–P2 2.424(9) Å] and partecipates with P1 to the chelation of Ru2 [Ru2–P1 2.384(10), Ru2–P2 2.424(9) Å]. The migratory insertion of a phenyl ring into the C7–O7 carbonyl group causes the elongation of Ru–C and C–O bond distances [2.01(4) an 1.27(4) Å, respectively] and the formation of a benzoyl moiety bridging the Ru3 and Ru1 atoms through C7 and O7 atoms, respectively. A similar structure has been observed in $[Ru_3(\mu_3\text{-}Se)\{\mu\text{-}P(Ph)C_5H_4FeC_5H_4PPh_2\}(\mu\text{-}OCPh)(CO)_6]$ [32] showing a Ru_3Se core.

4. Supplementary material

Crystallographic data for the structural analysis have been deposited with the Cambridge Crystallographic Data Centre, CCDC Nos. 185511–185514 compounds **3**, $\mathbf{2}\cdot 0.5CH_2Cl_2$, $\mathbf{1}\cdot 0.5CHCl_3$ and **4**, respectively. Copies of this information may be obtained free of charge from The Director, CCDC, 12 Union Road, Cambridge, CB2 1EZ, UK (fax: +44-1223-336-033; e-mail: deposit@ccdc.cam.ac.uk or www: http://www.ccdc.cam.ac.uk).

Acknowledgements

Financial support from the Ministero dell'Università e della Ricerca Scientifica e Tecnologica (Roma, Cofin 2000) is gratefully acknowledged. The facilities of the Centro Interdipartimentale di Misure (Università di Parma) were used to record the NMR and mass spectra.

References

[1] L.C. Roof, J.W. Kolis, Chem. Rev. 93 (1993) 1037.
[2] G. Schmid (Ed.), Cluster and Colloids, Ch. 3, VCH, Weinheim, 1994.
[3] S. Dehnen, A. Eichhöfer, D. Fenske, Eur. J. Inorg. Chem. (2002) 279.
[4] M.L. Steigerwald, Polyhedron 13 (1994) 1245.
[5] H. Weller, Angew. Chem., Int. Ed. Engl. 32 (1993) 41.
[6] M.M. Kappes, Chem. Rev. 88 (1988) 369.
[7] D. Cauzzi, C. Graiff, G. Predieri, A. Tiripicchio, in: P. Braunstein, L. Oro, P. Raithby (Eds.), Metal Cluster in Chemistry, vol. 1, VCH, Weinheim, 1999, p. 193.
[8] P. Baistrocchi, D. Cauzzi, M. Lanfranchi, G. Predieri, A. Tiripicchio, M. Tiripicchio Camellini, Inorg. Chim. Acta 235 (1995) 173.
[9] D. Cauzzi, C. Graiff, C. Massera, G. Predieri, A. Tiripicchio, D. Acquotti, J. Chem. Soc., Dalton Trans. (1999) 3515.
[10] D. Cauzzi, C. Graiff, M. Lanfranchi, G. Predieri, A. Tiripicchio, J. Chem. Soc., Dalton Trans. (1995) 2321.
[11] D. Cauzzi, C. Graiff, C. Massera, G. Predieri, A. Tiripicchio, Inorg. Chim. Acta. 300–302 (2000) 471.
[12] D. Cauzzi, C. Graiff, C. Massera, G. Predieri, A. Tiripicchio, J. Cluster Sci. 12 (2001) 259.
[13] D. Cauzzi, C. Graiff, C. Massera, G. Predieri, A. Tiripicchio, Eur. J. Inorg. Chem. (2001) 721.
[14] P. Braunstein, C. Graiff, C. Massera, G. Predieri, J. Rosé, A. Tiripicchio, Inorg. Chem. 41 (2002) 1372.
[15] P. Braunstein, J. Rosé, in: P. Braunstein, L.A. Oro, P.R. Raithby (Eds.), Metal Clusters in Chemistry, vol. 2, VCH, Weinheim, 1999, pp. 616–677.
[16] P. Braunstein, E. Sappa, A. Tiripicchio, Coord. Chem. Rev. 65 (1985) 219.
[17] W. Imhof, G. Huttner, J. Organomet. Chem. 448 (1993) 247.
[18] S. Vastag, G. Gervasio, D. Marabello, G. Szalontai, L. Marko, Organometallics 17 (1998) 4218.
[19] G. Hogarth, N.J. Taylor, A.J. Carty, A. Meyer, J. Chem. Soc., Chem. Commun. (1988) 834.
[20] A.M. Aguiar, M.G.R. Nair, J. Org. Chem. 33 (1968) 579.
[21] H. Werner, M. Ebner, W. Bertleff, U. Schubert, Organometallics 2 (1983) 891.
[22] A.J. Paviglianiti, D.J. Minn, W.C. Fultz, J.L. Burmeister, Inorg. Chim. Acta 159 (1989) 65.

[23] M. Ebner, H. Otto, H. Werner, Angew. Chem., Int. Ed. Engl. 24 (1985) 518.
[24] H. Werner, M. Ebner, H. Otto, J. Organomet. Chem. 350 (1988) 257.
[25] M. Camalli, F. Caruso, S. Chaloupka, E.M. Leber, H. Rimml, L.M. Venanzi, Helv. Chim. Acta 73 (1990) 2263.
[26] F. Caruso, M. Camalli, H. Rimml, L.M. Venanzi, Inorg. Chem. 34 (1995) 673.
[27] SMART Software Users Guide, version 5.1, Bruker Analytical X-ray Systems, Madison, WI, 1999.
[28] SAINT Software Users Guide, version 6.0, Bruker Analytical X-ray Systems, Madison, WI, 1999.
[29] G.M. Sheldrick, SADABS, Bruker Analytical X-ray Systems, Madison, WI, 1999.
[30] G.M. Sheldrick, SHELXTL v5.1: Program for the Refinement of Crystal Structures 97-2, University of Göttingen, Göttingen, Germany, 1998.
[31] M. Careri, C. Graiff, A. Mangia, P. Manini, G. Predieri, Rapid Commun. Mass Spectrom. 12 (1998) 225–230.
[32] F. Fabrizi de Biani, C. Graiff, G. Opromolla, G. Predieri, A. Tiripicchio, P. Zanello, J. Organomet. Chem. 637–639 (2001) 586.
[33] D. Cauzzi, C. Graiff, G. Predieri, A. Tiripicchio, C. Vignali, J. Chem. Soc., Dalton Trans. (1999) 237.
[34] P. Baistrocchi, M. Careri, D. Cauzzi, C. Graiff, M. Lanfranchi, P. Manini, G. Predieri, A. Tiripicchio, D. Acquotti, Inorg. Chim. Acta 252 (1996) 367.
[35] D. Cauzzi, C. Graiff, M. Lanfranchi, G. Predieri, A. Tiripicchio, J. Organomet. Chem. 536-537 (1997) 497.